Inorg. Chem. **2007**, *46*, 9030–9032

Metal-Based Netropsin Mimics Showing AT-Selective DNA Binding and DNA Cleavage Activity at Red Light

Ashis K. Patra,[†] Tuhin Bhowmick,[‡] Suryanarayanarao Ramakumar,[‡] and Akhil R. Chakravarty*,[†]

Department of Inorganic and Physical Chemistry, and Bioinformatics Center, Department of Physics, Indian Institute of Science, Bangalore-560012, India

Received July 4, 2007

Copper(II) bis-arginate $[Cu(L\text{-arg})_2](NO_3)_2$ (**1**) and [Cu(L-arg)(phen)Cl]Cl (**2**) as mimics of the minor-groove-binding natural antibiotic netropsin show preferential binding to the AT-rich region of double-stranded DNA. The complexes with a d–d band near 600 nm display oxidative DNA cleavage activity on photoirradiation at UV-A light of 365 nm and at red light of 647.1 nm (Ar–Kr laser) in a metal-assisted photoexcitation process forming singlet oxygen ($^1O_2$) species in a type-2 pathway.

Photodynamic therapy (PDT) is an emerging method of noninvasive treatment of cancer in which drugs like Photofrin shows localized toxicity on photoactivation at the tumor cells leaving the healthy cells unaffected.[1−4] The importance of PDT has necessitated a search for new photosensitizers that could show selective binding to DNA and photoactivation within the PDT window of 630−800 nm.[5−8] Sequence-specific DNA minor-groove-binding molecules like netropsin (ntp) and distamycin (dst) are antiviral antibiotics used extensively for biomedical applications for their selective binding to the AT-rich sequences of DNA.[9−11] Both ntp and dst with a crescent-shaped structure are efficient binders to DNA and exert significant biological activity by interfering with the proteins that regulate replication and transcription processes. The molecules, however, lack any electronic spectral band in the PDT window. As a consequence, they in unmodified form or their amino acids/peptide analogues cleave DNA only at UV light and are not suitable for PDT applications.[9]

Scheme 1 . Netropsin (ntp) in Diprotonated Form, $[Cu(L\text{-arg})_2]^{+2}$ (**1**) and the Perspective View of $[Cu(L\text{-arg})(phen)Cl]^+$ (**2**) Showing Crescent-Shaped Structures

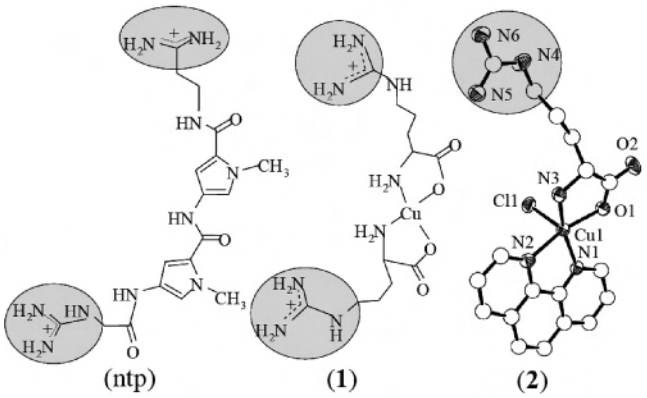

Netropsin derivatives bound to transition metal ions are known to show "chemical nuclease" and/or hydrolase activities.[9,12−14] To circumvent the predicament of photocleavage in the PDT window, we have chosen the crescent-shaped copper(II) bis-arginate complex as a structural mimic of netropsin, having end group similarities along with its analogue [Cu(L-arg)(phen)Cl]Cl (**2**) having 1,10-phenanthroline as a DNA binder (Scheme 1). The water-soluble complexes $[Cu(L\text{-arg})_2](NO_3)_2$ (**1**) and **2** have $3d^9$ copper(II) bound to L-arginine ligand with a pendant guanidinium terminal moiety.

Complex **1** is prepared and characterized following a literature method.[15] It has a square-planar geometry with the

* To whom correspondence should be addressed. E-mail: arc@ipc.iisc.ernet.in. Tel: 91-80-22932533. Fax: 91-80-23600683.
† Department of Inorganic and Physical Chemistry.
‡ Bioinformatics Center, Department of Physics.

(1) Bonnet, R. *Chemical Aspects of Photodynamic Therapy*; Gordon and Breach: London, U.K., 2000.
(2) Henderson, B. W.; Busch, T. M.; Vaughan, L. A.; Frawley, N. P.; Babich, D.; Sosa, T. A.; Zollo, J. D.; Dee, A. S.; Cooper, M. T.; Bellnier, D. A.; Greco, W. R.; Oseroff, A. R. *Cancer Res.* **2000**, *60*, 525.
(3) Sternberg, E. D.; Dolphin, D.; Brückner, C. *Tetrahedron* **1998**, *54*, 4151.
(4) Ali, H.; van Lier, J. E. *Chem. Rev.* **1999**, *99*, 2379.
(5) Chifotides, H. T.; Dunbar, K. R. *Acc. Chem. Res.* **2005**, *38*, 146.
(6) Atilgan, S.; Ekmekci, Z.; Dogan, A. L.; Guc, D.; Akkaya, E. U. *Chem. Commun.* **2006**, 4398.
(7) Magda, D. J.; Wang, Z.; Gerasimchuk, N.; Wei, W.; Anzenbacher, P.; Sessler, J. L. *Pure Appl. Chem.* **2004**, *76*, 365.
(8) Rodriguez, M. E.; Moran, F.; Bonansea, A.; Monetti, M.; Fernandez, D. A.; Strassert, C. A.; Rivarola, V.; Awruch, J.; Dicelio, L. E. *Photochem. Photobiol. Sci.* **2003**, *2*, 988.
(9) Bailly, C.; Chaires, J. B. *Bioconj. Chem.* **1998**, *9*, 513.
(10) Neidle, S. *Nat. Prod. Rep.* **2001**, *18*, 291.
(11) Zimmer, Z.; Wähnert, U. *Prog. Biophys. Mol. Biol.* **1986**, *47*, 31.
(12) Chiang, S.-Y.; Welch, J.; Rauscher, F. J.; Beerman, T. A. *Biochemistry* **1994**, *33*, 7033.
(13) Welch, J. J.; Rauscher, F. J.; Beerman, T. A. *J. Biol. Chem.* **1994**, *269*, 31051.
(14) Schultz, P. G.; Dervan, P. B. *Proc. Natl. Acad. Sci. U.S.A.* **1983**, *80*, 6834.
(15) Masuda, H.; Odani, A.; Yamazaki, T.; Yajima, T.; Yamauchi, O. *Inorg. Chem.* **1993**, *32*, 1111.

10.1021/ic701326z CCC: $37.00
Published on Web 09/20/2007

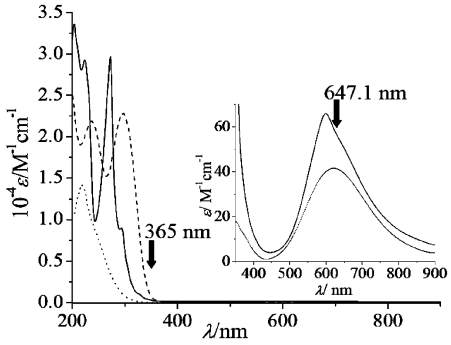

Figure 1. Electronic spectra of netropsin dihydrochloride (− − −), **1** (· · ·) and **2** (—) in aqueous medium. Inset shows the d−d band of the copper(II) complexes and the wavelength of photoirradiation.

ligands in a cis configuration. The aqueous solution of the complex displays a d−d band at 630 nm and a ligand-centered band at 217 nm, whereas netropsin shows two electronic spectral bands at 237 and 297 nm (Figure 1). Complex **2**, prepared from a reaction of L-arginine with $CuCl_2{\cdot}2H_2O$ and phen in aqueous methanol, has been structurally characterized by X-ray crystallography.[16,17] The crystal structure of **2** shows a bidentate N,O-binding mode of L-arginine with a pendant positively charged guanidinium moiety and a N,N-donor 1,10-phenanthroline in a square pyramidal (4 + 1) geometry having an axial chloride ligand (Scheme 1). Complex **2** displays a d−d band at 600 nm and ligand-centered bands within 220−290 nm. The redox active complexes show the Cu(II)/Cu(I) couple at −0.38 V vs SCE (ΔE_p = 330 mV) for **1** and at −0.12 V (ΔE_p = 310 mV) for **2** at 50 mV s^{-1} in DMF/0.1 M $[Bu_4N](ClO_4)$.

The mode and propensity of binding of netropsin, **1** and **2** to calf thymus (CT) DNA have been studied using spectral, DNA melting, and viscosity measurements. For sequence

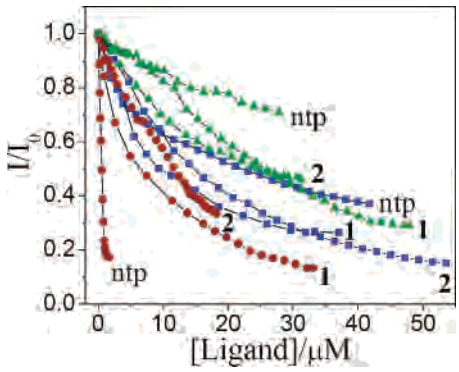

Figure 2. Effect of increasing the concentration of netropsin (ntp), **1** and **2** on the emission intensity of ethidium bromide bound poly(dA).poly(dT) (●), CT-DNA (■), and poly(dG).poly(dC) (▲) in 5 mM Tris buffer-5 mM NaCl medium. K_{app} values for ntp, **1** and **2** are 6.1 × 10^6,1.3 × 10^6, 9.3 × 10^5 with CT-DNA; 2.3 × 10^7, 1.5 × 10^6, 1.1 × 10^6 with poly(dA)·poly(dT), and 1.8 × 10^5, 5.3 × 10^5, 4.9 × 10^5 M^{-1} with poly(dG)·poly(dC).

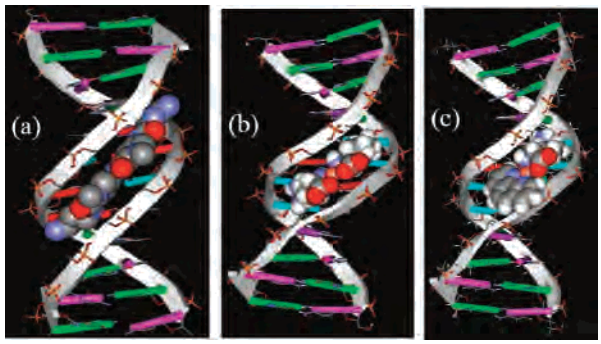

Figure 3. View of the crystal structure of netropsin bound to d(CGC-GAATTCGCG) [NDB Code: GDLB05] (a). View of the energy minimized docked structure of **1** (b) and **2** (c) with d(CGCGAATTCGCG).

selectivity of the complex, we have carried out binding study using synthetic oligomers poly(dA)·poly(dT) and poly(dG)·poly(dC) (Figure 2). The equilibrium binding constant (K_b) and the binding site size (*s*) values obtained from the nonlinear least-squares fitting are 7.0(±0.1) × 10^5 M^{-1} and 0.12 for **1**; 1.2(±0.1) × 10^5 M^{-1} and 0.6 for **2**, and 2.0-(±0.1) × 10^6 M^{-1} and 0.3 for netropsin with CT-DNA.[18] The complexes and netropsin show preferential binding to poly(dA)·poly(dT) in comparison to poly(dG)·poly(dC). Molecular docking calculations have been carried out to investigate the binding interaction of **1** and **2** with d(CGC-GAATTCGCG) dodecamer (Figure 3). The results show binding of **1** to the phosphate backbone of the polynucleotide involving the terminal positively charged guanidinium end groups of arginine through H-bonding (2.8−3.0 Å) and ionic contacts (Figure 3b).[19] The complex preferentially binds at the AT region of the dodecamer. The span of AT-binding stretch is relatively short compared to netropsin due to shorter overall length of the complex. This finding is consistent with the binding parameters obtained from the spectroscopic titration. The optimal binding conformation in the AT stretches of minor groove forms an extensive H-bonding

(16) Complex **2** was prepared from a reaction of $CuCl_2.2H_2O$ (0.17 g, 1.0 mmol) with an aqueous solution of L-arginine (0.23 g, 1.1 mmol) treated with NaOH (0.04 g, 1.0 mmol) and followed by slow addition of a methanolic solution of 1,10-phenanthroline (0.18 g, 0.9 mmol). The reaction mixture was stirred at 25 °C for 2 h and filtered. The filtrate on slow evaporation gave blue, rectangular-shaped single crystals suitable for X-ray diffraction. The crystals were isolated and washed with aqueous methanol (1:1 v/v) before drying over P_4O_{10} [Yield: ∼75%]. The complex showed good solubility in water, methanol, ethanol, *N*,*N*-dimethylformamide (DMF), and dimethyl sulfoxide (DMSO). The ternary structure is stable in solution. Anal. Calcd for $C_{18}H_{22}Cl_2CuN_6O_2$ (**2**): C, 44.22; H, 4.54; N, 17.19. Found: C, 44.12; H, 4.45; N, 16.94. IR (KBr phase): 3373br, 3194br, 3027br, 1684s, 1660vs, 1601s, 1477m, 1445s, 1378s, 1343m, 1156m, 1031w, 769s, 730m, 572m, 414m cm^{-1} (br, broad; s, strong; vs, very strong; m, medium; w, weak). UV-vis in H_2O [λ_{max}, nm (ϵ, M^{-1} cm^{-1})]: 204 (33 600), 223 (29 300), 273 (29 700), 294 (9000), and 600 (70). ESI-MS in H_2O-MeCN: *m*/*z* 458 $[M - 2Cl + MeCN]^+$, 452 $[M - Cl]^+$. μ_{eff} (298 K): 1.76 μ_B.

(17) Crystal data for **2**·$2.5H_2O$: $C_{18}H_{27}Cl_2CuN_6O_{4.5}$, M = 533.90, triclinic, space group $P1$ (No. 1), a = 10.359(6) Å, b = 12.437(7) Å, c = 18.888(11) Å, α = 94.599(9)°, β = 104.701(9)°, γ = 101.002(9)°, V = 2289(2) $Å^3$, Z = 4, ρ = 1.549 g cm^{-3}, T = 293(2) K, 1.89° ≤ θ ≤ 26.00°, μ = 12.27 cm^{-1}, $F(000)$ = 1104, R1 = 0.0454, wR2 = 0.1226 for 14 046 reflections with $I > 2\sigma(I)$ and 1136 parameters [R1-(F^2) = 0.0588 (all data)]. Weighting scheme: $w = 1/[\sigma^2 (F_o^2) + (0.0823P)^2 + 0.0P]$, where $P = [F_o^2 + 2F_c^2]/3$. The GOF and the largest difference peak were 1.025 and 0.934 e $Å^{-3}$, respectively. Perspective view of the complex was obtained by ORTEP. Data were collected using Bruker SMART APEX CCD diffractometer with a Mo Kα X-ray source. The structure was solved and refined using the *SHELX* program (Sheldrick, G. M. *SHELX-97, Programs for Crystal Structure Solution and Refinement*; University of Göttingen: Göttingen, Germany,1997).

(18) Carter, M. T.; Rodriguez, M.; Bard, A. J. *J. Am. Chem. Soc.* **1989**, *111*, 8901. K_b (*s*) values for ntp, **1** and **2** are 4.2 × 10^6 (0.34), 1.8 × 10^6 (0.24), 2.6 × 10^6 (0.49) with poly(dA)·poly(dT) and 6.0 × 10^5 (1.2), 3.4 × 10^5 (0.28), 9.3 × 10^4 (0.27) M^{-1} with poly(dG)·poly-(dC), respectively. The ΔT_m values for ntp, **1** and **2** are 18, 3, 2 with CT-DNA and 38, 11, 8 °C with poly(dA)·poly(dT), respectively.

network with the A and T base pairs of B-DNA. This establishes that the crescent-shaped backbone structure of the molecule is important to bind efficiently with the DNA in the minor groove. Complex **2** also shows favorable H-bonding interactions with the AT base pair sequences of ds-DNA and positively charged guanidinium end group (2.7−3.0 Å). In addition, phen makes favorable stacking interaction with the DNA base pairs (Figure 3c).

The photonuclease activity of netropsin and the complexes is studied using supercoiled (SC) pUC19 DNA in a medium of Tris-HCl/NaCl buffer (pH 7.2) on photolysis at UV-A light of 365 nm and red light of 647.1 nm (Ar−Kr mixed gas−ion laser).[20] The extent of DNA cleavage is measured by agarose gel electrophoresis on the basis of the conversion of the SC to its nicked circular (NC) and linear form of DNA. A 50 μM solution of **1** shows complete cleavage of SC DNA (30 μM) on photoexposure at 365 nm for 1 h with significant formation of linear DNA. A 10 μM solution of **2** shows complete cleavage of DNA under similar conditions. Complexes **1** and **2** differ in their DNA cleavage activity at red light. While complex **1** is a poor cleaver of DNA at 647.1 nm, complex **2** shows significant cleavage activity (Figure 4a, lane 13). Netropsin is cleavage inactive at red light. The cleavage of DNA at red light is believed to occur in a metal-assisted photoactivation process involving the d−d band.[21,22]

The mechanistic aspects of the DNA cleavage reaction are studied using different reagents (Figure 4b). Complexes **1** and **2** are cleavage inactive in the presence of netropsin or distamycin-A, suggesting their minor groove binding preference. A complete inhibition of DNA cleavage takes place under argon. Inhibition of cleavage in the presence of singlet oxygen quencher NaN_3 and enhancement of cleavage in D_2O indicate the involvement of $^1O_2$ as the reactive species.[23,24] Addition of respective $HO^\bullet$ radical, H_2O_2, and $O_2^{\bullet-}$ radical

Figure 4. (a) Gel electrophoresis diagram showing photoinduced oxidative cleavage of SC pUC19 DNA (0.2 μg, 30 μM) by netropsin (ntp, 50 μM), **1** (50 μM) and **2** (10 μM) at UV light of 365 nm (lanes 1, 4−10, 1h exposure) and red light of 647.1 nm (lanes 11−13, 2h exposure): lane 1, DNA control; lane 2, DNA + **1** (in dark); lane 3, DNA + **2** (in dark); lane 4, DNA + L-arg (50 μM); lane 5, DNA + $CuCl_2 \cdot 2H_2O$ (50 μM); lane 6, DNA + ntp; lane 7, DNA + **1**; lane 8, DNA + **2**; lane 9, DNA + ntp + **1**; lane 10, DNA + ntp + **2**; lane 11, DNA + ntp; lane 12, DNA + **1**; lane 13, DNA + **2**. (b) Gel electrophoresis diagram showing photoinduced cleavage of SC pUC19 DNA (0.2 μg, 30 μM) by **2** (50 μM) at red light of 647.1 nm for 2h exposure time: lane 1, DNA control; lane 2, DNA + **2**; lane 3, DNA + $[Cu(phen)_2]^{2+}$ (50 μM); lane 4, DNA + **2** (under Ar); lane 5, DNA + NaN_3 (100 μM) + **2**; lane 6, DNA + D_2O (16 μL) + **2**; lane 7, DNA + DMSO (2 μL) + **2**; lane 8, DNA + catalase (4 units)+ **2**; lane 9, DNA + SOD (4 units) + **2**.

scavengers DMSO, catalase, and SOD do not show any apparent effect on the photocleavage activity in UV and red light. The photocleavage reaction at 365 and 647.1 nm proceeds via singlet oxygen pathway (type-II process).

In conclusion, we report here the first metal-based netropsin mimics showing efficient AT-selective DNA binding and photoinduced DNA cleavage activity at red light. The oxidative photocleavage of DNA in the PDT window occurs in a metal-assisted photosensitization process involving the d−d band forming singlet oxygen as the reactive species. The results are of significance as highly specific cell-permeable metal-based natural antibiotic analogues/mimics suitable for binding at the AT stretches can be tailored for potential PDT applications. Further work in that direction is currently in progress.

Acknowledgment. We thank the Department of Science and Technology, Government of India, for financial support and a CCD difractometer facility. A.K.P. and T.B. are grateful to CSIR, New Delhi, for research fellowships. We thank the AvH Foundation, Germany, for an electrochemical system.

Supporting Information Available: Crystallographic details in CIF format, ORTEP view (Figure S1), unit cell packing diagram (Figure S2), space filling model of the complexes (Figure S3), cyclic voltammograms (Figure S4), theoretical calculation details and corresponding figure (Figure S5), DNA binding plots (Figures S6−S10) and gel electrophoresis diagrams (Figures S11, S12), and ESI-MS of complex **2** (Figure S13). This material is available free of charge via the Internet at http://pubs.acs.org.

IC701326Z

(19) Molecular docking calculation was done using the DS Modelling, 1.2-SBD Docking Module by Accelrys Software. The CHARMm force-field was used for the metal complexes. The crystal structure of the B-DNA dodecamer, $d(CGCGAATTCGCG)_2$ (NBD code GDLB05) was obtained from the protein data bank. Some important H-bonding parameters (Å) for **1** in the docked state are H(N8)−O(A19), 2.65; H(N13)−O(T6), 2.78 (Figure S5a); in **2**: H(N12)−O(T6), 2.96; H(N5)−O3(A20), 2.68; H(N9)−N3(A20), 3.04 (Figure S5b). Mondal, S.; Vijayan, R.; Shichina, K.; Babu, R. M.; Ramakumar, S. *In Silico Biol.* **2005**, *5*, 557.

(20) Photo-induced DNA cleavage experiments were done using supercoiled (SC) pUC19 DNA (0.2 μg, 30 μM bp) in 5 mM Tris-HCl/5 mM NaCl buffer (pH 7.2). The light sources used were UV lamp of 365 nm (12 W) and Spectra Physics Water-Cooled Mixed-Gas Ion Laser Stabilite 2018-RM with Laser Power Meter Model 407A for 647.1 nm wavelength (100 mW laser power at the sample position, continuous-wave (CW) beam diameter at $1/e^2$ 1.8 mm ± 10%, beam divergence 0.7 mrad ± 10%). The complex and reagent concentrations correspond to those in the 20 μL sample volume (solution path-length = 5 mm). The extent of DNA cleavage was measured from the intensities of the bands in agarose gels using UVITECH Gel Documentation System giving an intensity measurement error of ~5%.

(21) Patra, A. K.; Nethaji, M.; Chakravarty, A. R. *Dalton Trans.* **2005**, 2798.

(22) Dhar, S.; Senapati, D.; Das, P. K.; Chattopadhyay, P.; Nethaji, M.; Chakravarty, A. R. *J. Am. Chem. Soc.* **2003**, *125*, 12118.

(23) Szacilowski, K.; Macyk, W.; Drzewiecka-Matuszek, A.; Brindell, M.; Stochel, G. *Chem. Rev.* **2005**, *105*, 2647.

(24) Armitage, B. *Chem. Rev.* **1998**, *98*, 1171.